

The parameter identification model considering both geometric parameters and joint stiffness

Jing Bai, Le Fan and Shuyang Zhang

School of Mechanical Engineering, Northwestern Polytechnical University, Xi'an, China

Zengcui Wang

Hisense Electric Appliance Co. Ltd, Qingdao, China, and

Xiansheng Qin

School of Mechanical Engineering, Northwestern Polytechnical University, Xi'an, China

Abstract

Purpose – Both geometric and non-geometric parameters have noticeable influence on the absolute positional accuracy of 6-dof articulated industrial robot. This paper aims to enhance it and improve the applicability in the field of flexible assembling processing and parts fabrication by developing a more practical parameter identification model.

Design/methodology/approach – The model is developed by considering both geometric parameters and joint stiffness; geometric parameters contain 27 parameters and the parallelism problem between axes 2 and 3 is involved by introducing a new parameter. The joint stiffness, as the non-geometric parameter considered in this paper, is considered by regarding the industrial robot as a rigid linkage and flexible joint model and adds six parameters. The model is formulated as the form of error via linearization.

Findings – The performance of the proposed model is validated by an experiment which is developed on KUKA KR500-3 robot. An experiment is implemented by measuring 20 positions in the work space of this robot, obtaining least-square solution of measured positions by the software MATLAB and comparing the result with the solution without considering joint stiffness. It illustrates that the identification model considering both joint stiffness and geometric parameters can modify the theoretical position of robots more accurately, where the error is within 0.5 mm in this case, and the volatility is also reduced.

Originality/value – A new parameter identification model is proposed and verified. According to the experimental result, the absolute positional accuracy can be remarkably enhanced and the stability of the results can be improved, which provide more accurate parameter identification for calibration and further application.

Keywords Robot calibration, Joint stiffness, Laser tracker, Parameter identification model

Paper type Technical paper

1. Introduction

Because of the characteristics of dexterity, high automation, good flexibility and low cost (Wang *et al.*, 2018; Chen *et al.*, 2017), the industrial robot, as the most typical mechatronic digital equipment, is more and more widely applied in the field of precision work such as automatic assembly, drilling and riveting, dimension inspections and laser machining. Meanwhile, due to the increasing requirements of the complexity and flexibility of the industrial robot operation and frequent usages in the real-time applications (Bo *et al.*, 2014), the off-line programming technology has become a hotspot in the robot technology. However, although the repeatability accuracy of the industrial robot can be high enough, the absolute positioning accuracy is rather low (For instance, the repeatability accuracy of KUKA KR500-3 type robot is 0.08 mm but the absolute accuracy only reaches to centimeter-

level.), which severely restricts the popularization and application of the robot off-line programming technology.

To improve the absolute positional accuracy and promote the practicability of off-line programming, the robot calibration is the main technology, which contains the processes of modeling, measurement, parameter identification and compensation (Ren *et al.*, 2007). Among these steps, the parameter identification is a crucial part, which divides the identification into two types, geometric parameter calibration and the non-geometric parameter calibration (Nubiola and Bonev, 2013), based on the different types of identification

© Jing Bai, Le Fan, Shuyang Zhang, Zengcui Wang and Xiansheng Qin. Published by Emerald Publishing Limited. This article is published under the Creative Commons Attribution (CC BY 4.0) licence. Anyone may reproduce, distribute, translate and create derivative works of this article (for both commercial and non-commercial purposes), subject to full attribution to the original publication and authors. The full terms of this licence may be seen at <http://creativecommons.org/licences/by/4.0/legalcode>

This work is partially supported by the National Science Foundation for Young Scientists of China (Grant No. 51805438) and the “111 project” of China (Grant No. B13044).

Received 1 November 2018

Revised 17 June 2019

Accepted 27 June 2019

The current issue and full text archive of this journal is available on Emerald Insight at: <https://www.emerald.com/insight/0143-991X.htm>



Industrial Robot: the international journal of robotics research and application
47/1 (2020) 76–81
Emerald Publishing Limited [ISSN 0143-991X]
[DOI 10.1108/IR-11-2018-0223]

parameters. According to Zhong and Lewis (1995), Liou *et al.* (1993), as well as Ziegert (1988), the factors that affect the absolute positioning accuracy of the industrial robot are multitudinous, consisting of geometric factors that include the structure parameter error caused by assembly and manufacturing process, zero deviation and specific applications (end effector installation), as well as non-geometric factors that include environmental factors such as the temperature, kinetic parameters, stiffness, backlash and other nonlinearities. On account of the lower stiffness, the absolute positioning errors of industrial robots caused by compliance errors due to the external load cannot be neglected.

However, most traditional calibration technologies for industrial robots are limited to studying the influence of a single factor on the absolute positioning accuracy of the robot and ignore the coupled effect of various factors on this accuracy. Chen *et al.* (2008) developed a convenient and practical method which only calculated the zero offset. Considering the robot end-effector errors, Joubair *et al.* (2016) developed an analysis to determine the most appropriate observability index, which allowed for the best parameter identification, and Oh (2018) proposed a method to analyze the robot geometric error by using the data measured during circle contouring movement of the industrial robot end effectors. Besides the research related to geometric parameters, there are also many studies considering non-geometric parameters. On the premise of neglecting the error from geometric parameters, Chen (2011) and Wang *et al.* (2009) analyzed and identified the robot joint stiffness. Based on the calibration modeling of relative positioning accuracy and the identification of geometric parameters, Wang *et al.* (2011) proposed a method to compensate the compliance error of the external load and self-weight. He *et al.* (2017) identified the geometric parameters based on kinematics parameter calibration and proposed a method of compensation for residual error based on error similarity. Filion *et al.* (2018) applied a portable photogrammetry system to proceed the elasto-geometrical model and parameter identification. Considering both geometric and non-geometric parameters, Karan and Vukobratovic (2009) elaborated a joint-stiffness identification model but did not display the specific model.

According to the literature, there are a few researches integrated considering the geometric and non-geometric parameters into the identification and calibration. Therefore, to remove the coupled effect of multi-factors on positioning accuracy and improve it, this paper proposes a more practical parameter identification model which considers geometric parameter errors and compliance errors caused by external loads. Based on the proposed model, a calibration experiment on KUKA robot KR500-3 is performed and the result analysis verifies that the proposed model can enhance the absolute positioning accuracy and reduce the volatility at the same time.

2. Kinematics model of the 6R robot

Based on the classical DH coordinate system, the kinematics model is set up, which is shown in Figure 1. The robot theoretical DH parameters are shown in Table I. The robot used in this paper is KUKA KR500-3 type robot, whose payload, arm length and repeatability are $500 \pm 50\text{kg}$,

Figure 1 KR 500-3 robot and its coordinate system

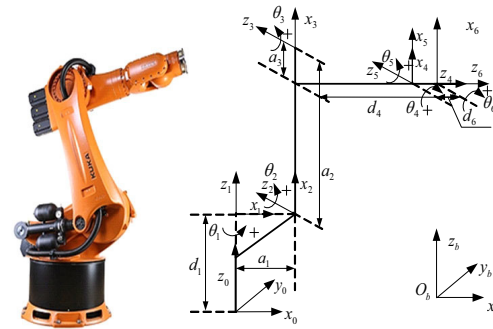


Table I Theoretical DH parameters of KR 500-3

link i	$\theta_i(\circ)$	d_i (mm)	a_{i-1} (mm)	$\partial_{i-1}(\circ)$	$\theta_i(\circ)$
1	$\theta_1(0)$	$d_1(1045)$	0	0	$-185 \sim 185$
2	$\theta_2(-90)$	0	$a_1(500)$	-90	$-130 \sim 20$
3	$\theta_3(0)$	0	$a_2(1300)$	0	$-100 \sim 144$
4	$\theta_4(0)$	$d_4(1025)$	$a_3(-55)$	-90	$-350 \sim 250$
5	$\theta_5(0)$	0	0	90	$-120 \sim 120$
6	$\theta_6(0)$	d_6	0	-90	$-350 \sim 350$

2826 mm and 0.08 mm, respectively. Some specific values of parameters of this robot are also shown in Table I.

3. Positional error model

3.1 Geometric and non-geometric factors

The positioning error of industrial robots is composed of a variety of geometric and non-geometric factors, where the linkage deformations and joint deformations of robots caused by external loads need to be considered in most cases. For most industrial robots, the joint deformation caused by inadequate joint stiffness is the main part, which results in the positioning error. Thus, an important assumption is made that the industrial robot is regarded as a rigid linkage and flexible joint model, namely neglecting the linkage deflection caused by external loads.

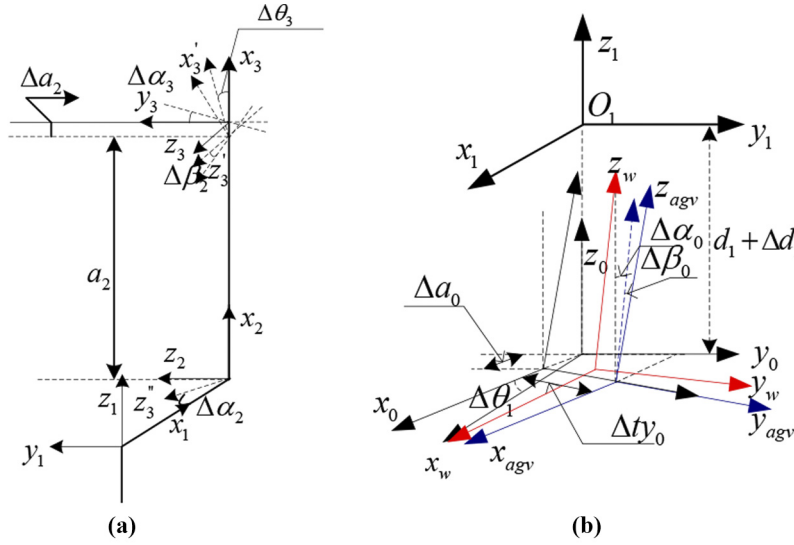
According to this assumption, each joint can be treated as an elastic torsion spring that its elasticity coefficient is constant (Wang *et al.*, 2009), and the error which is introduced by the insufficient stiffness is concretized as the joint angle error. Thus, the total angle error can be expressed as

$$\Delta\theta = \Delta\theta_s + \Delta\theta_p + \Delta\theta_{etc} \quad (1)$$

where $\Delta\theta_s$ and $\Delta\theta_p$ represent the joint angle error caused by the joint stiffness and geometric factors, respectively. $\Delta\theta_{etc}$ is the error caused by other factors which is neglected.

For the error caused by geometric parameters, the traditional DH parameters are not applicable when the axis 2 and axis 3 of the robot are nominal parallel. Thus, a parameter β , the twist angle along direction y , is introduced. Because of the installation error or other relative effects, an angle $\Delta\beta_2$ which is usually in a small scale is introduced between the axis 2 and axis 3, which is along the direction of y_2 (according to the right hand rule), shown in Figure 2(a).

Figure 2 Schematic of the error. $O-x_{agv}y_{agv}z_{agv}$: the constructed base coordinate system, $O-x_wy_wz_w$: the actual world coordinate system, $O-x_1y_1z_1$: the coordinate system of fixed axis 1 of robot



Notes: (a) The error between axis 2 and 3; (b) the error from the coordinate system

The x_i , y_i and z_i represent the coordinate direction. Instead of Δd_2 , the error of the joint distance which is set as $\Delta d_2 = 0$ under the condition, the $\Delta\beta_2$ is used to describe this deviation. Δa_2 is a distance deviation between axis z_2 and z_3 along the direction of x_2 . $\Delta\alpha_2$ is the angle deviation between axis z_2 and z_3 around the direction of x_2 .

When the positioning deviation is under measurement, the robot basic coordinate system ($O-x_{agv}y_{agv}z_{agv}$) is established that aims to overlap with the actual basic coordinate system ($O-x_wy_wz_w$). But it is impossible to make them coincident based on the existed technologies, which depends on the positioning accuracy and measurement accuracy. The error is shown as Figure 2(b). Thus, coordinate transformations are constructed, where ΔT_{aw} and ΔT_{w1} represent the transformation from the basic coordinate system to the actual base coordinate system and the transformation from the real robot base coordinate to the coordinate fixed to the axis 1 ($O-x_1y_1z_1$), respectively. To simplify the model, the error transformations can be expressed as:

$$\Delta T_{a1} = \Delta T_{aw} \cdot \Delta T_{w1} = \text{trans}(y_0, \Delta ty_0) \cdot \text{rot}(y_{agv}, \Delta\beta_0) \cdot \Delta T_{w1} \quad (2)$$

$$\Delta T_{w1} = \text{rot}(x, \Delta\alpha_0) \cdot \text{trans}(x, \Delta a_0) \cdot \text{rot}(z, \Delta\theta_1) \cdot \text{trans}(z, \Delta d_1) \quad (3)$$

where the six parameters describing the error are Δty_0 , $\Delta\beta_0$, $\Delta\alpha_0$, Δa_0 , $\Delta\theta_1$ and Δd_1 . Among these parameters, Δty_0 expresses the distance offset from the base coordinate to the actual robot coordinate system in the base coordinate system along the axis y_0 . $\Delta\beta_0$ expresses the angle deviation from z_{agv} to axis z_1 measured by z_{agv} . Other four parameters are defined according to the rule of DH parameter.

3.2 Geometric and non-geometric parameter model of positional error

Considering both geometric and non-geometric parameters, the total number of the robot error parameters is 33, which includes 27 geometric parameters and 6 stiffness parameters. For the specific KUKA KR500-3 robot, its error parameters are listed in Table II. Notably particularly, it is necessary to eliminate non-independent variables before calculating because of the correlation among parameters.

4. The parameter identification model considering joint stiffness

According to the kinematic model, when the joint angle θ is known, the nominal position is defined as:

$$P = F(a, d, \alpha, \theta) \quad (4)$$

where a is the joint deviation, d is the joint distance, and α is the joint twist angle. Meanwhile, considering the errors from both geometric and non-geometric parameters, the actual position is expressed as:

$$P' = F(a + \Delta a, d + \Delta d, \alpha + \Delta\alpha, \theta + \Delta\theta, \Delta\beta, \Delta ty_0, \Delta d_x) \quad (5)$$

Thus, the positioning error of robot can be expressed as:

$$\Delta P = P' - P \quad (6)$$

To simplify the expression into the linear equation when the involved parameters are relatively small, this error can be represented as:

Table II The Error parameters of KR 500-3

link <i>i</i>	Joint angle $\theta_i(\circ)$	Joint distance $d_i(mm)$	Joint deviation distance $a_{i-1}(mm)$	Joint twist angle $\partial_{i-1}(\circ)$	y-axis torsion angle $\Delta\beta_i(\circ)$
Structure Parameters					
1	$\theta_1 + \Delta\theta_{p1} + \Delta\theta_{s1}$	$d_1 + \Delta d_1$	Δa_0	$\Delta\partial_0$	0
2	$\theta_2 + \Delta\theta_{p2} + \Delta\theta_{s2}$	0	$a_1 + \Delta a_1$	$\Delta\partial_1 - 90^\circ$	$\Delta\beta_2$
3	$\theta_3 + \Delta\theta_{p3} + \Delta\theta_{s3}$	Δd_2	$a_2 + \Delta a_2$	$\Delta\partial_2$	0
4	$\theta_4 + \Delta\theta_{p4} + \Delta\theta_{s4}$	$d_4 + \Delta d_4$	$a_3 + \Delta a_3$	$\Delta\partial_3 - 90^\circ$	0
5	$\theta_5 + \Delta\theta_{p5} + \Delta\theta_{s5}$	Δd_5	Δa_4	$\Delta\partial_4 + 90^\circ$	0
6	$\theta_6 + \Delta\theta_6(\Delta A, \Delta\theta_{6s})$	$d_6 + \Delta d_6(\Delta t d_z)$	Δa_5	$\Delta\partial_5 - 90^\circ$	0
Tool Coordinate System					
System	$td_x + \Delta td_x$	$td_y + \Delta td_y$	$A + \Delta A$		
Positional Deviation	Δty_0				$\Delta\beta_0$

$$\Delta P = \mathcal{J} \cdot \Delta Q = \mathcal{J} \cdot (\Delta Q_s + \Delta Q_p) = \mathcal{J}_1 \cdot \Delta\theta_s + \mathcal{J} \cdot \Delta Q_p \quad (7)$$

$$\Delta P = A \cdot X \quad (15)$$

In this equation, \mathcal{J} is the Jacobian matrix which is the derivative of the tool center point (TCP) of the robot with respect to geometric parameters. And $\mathcal{J}_{1(3 \times 6)}$ is a part of the \mathcal{J} which includes the first six columns. ΔQ_s , ΔQ_p and ΔQ_s are respectively expressed as:

$$\Delta Q_s = [\Delta a, \Delta d, \Delta\alpha, \Delta\theta_p + \Delta\theta_s, \Delta\beta, \Delta y_0, \Delta t_x]^T \quad (8)$$

$$\Delta Q_p = [\Delta a, \Delta d, \Delta\alpha, \Delta\theta_p, \Delta\beta, \Delta y_0, \Delta t_x]^T \quad (9)$$

$$\Delta Q_s = [0, 0, 0, \Delta\theta_s, 0, 0, 0]^T \quad (10)$$

In the state of static equilibrium, the relationship between the external force of robot and the joint force is:

$$\Gamma = \mathcal{J}_f^T F_f \quad (11)$$

where Γ and F_f represent the external force and joint force, respectively. F_f contains both forces and torques, in the form as $[F_x, F_y, F_z, T_x, T_y, T_z]^T$, which are measured under the force coordinate system. \mathcal{J}_f is the 6×6 Jacobian matrix of the robot, calculated by using the differential transformation method. It describes the linear relationship between the velocity of TCP and the corresponding joint speed. With the relationship between the external force of robot and the joint force, the error $\Delta\theta_s$ can be represented as:

$$\Delta\theta_s = K_\theta^{-1} \Gamma = K_\theta^{-1} \mathcal{J}_f^T F_f = \text{diag}(\mathcal{J}_f^T F_f) \cdot C_\theta \quad (12)$$

where K_θ and C_θ are the stiffness matrix and the joint adaptation vector, respectively, which are expressed as:

$$K_\theta = \text{diag}[k_{\theta 1}, k_{\theta 2}, k_{\theta 3}, k_{\theta 4}, k_{\theta 5}, k_{\theta 6}] \quad (13)$$

$$C_\theta = [1/k_{\theta 1} \ 1/k_{\theta 2} \ 1/k_{\theta 3} \ 1/k_{\theta 4} \ 1/k_{\theta 5} \ 1/k_{\theta 6}]^T \quad (14)$$

Substituting (12) into (7), the absolute positional error is obtained as:

where

$$A = [\mathcal{J} \mathcal{J}_1 \cdot \text{diag}(\mathcal{J}_f^T F_f)], X = [dQ_p \ C_\theta]^T \quad (16)$$

When the measuring points are in the number of N , the error can be expressed as:

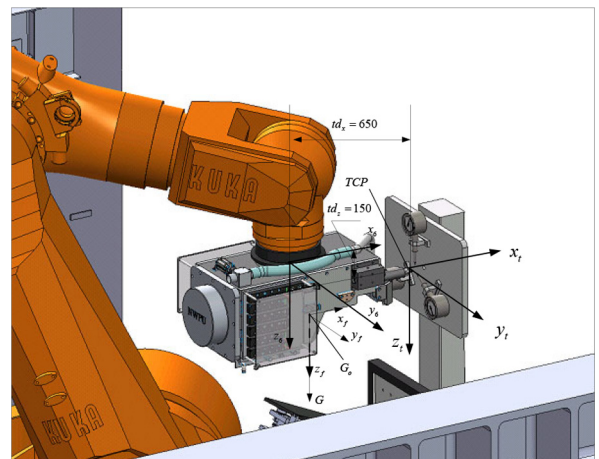
$$[\Delta P_1, \Delta P_2, \dots, \Delta P_N]^T = [A_1, A_2, \dots, A_N]^T \cdot X \quad (17)$$

Using the least square method, the least square solution of (15) is obtained, and the iteration makes ΔP verge to 0.

5. Experiment

To test the performance of the proposed model, an experiment is developed on KUKA KR500-3 type robot with an end effector which is 1103.58 N, shown as Figure 3. The absolute position of TCP is measured by laser tracker. The flange coordinate system is translated to the center of the gravity of end effector, then the force coordinate system is created and the vector F_f is defined upon it. Therefore, the value of the vector F_f changes with the posture of tool coordinate system. One thing should be noted is that the influence from self-weight is not considered.

Figure 3 The experiment equipment



Twenty groups of joint positions are selected and converted based on robot joint coordinates. Then, the converted locations are sent to robot and their actual positions are measured, which are listed in Table III. To guarantee the accuracy, each point is measured 5 times after the robot arrives at the position. The measured data are divided into two groups, where the data of the first 15 points are used for the construction of the model and the data of the last 5 points are used for testing the validity of the robot. Substituting the results in Table III to equation (17) and setting the iteration termination condition as:

$$\sum_{i=1}^{15} \left| \Delta p_{xi} \right| + \left| \Delta p_{yi} \right| + \left| \Delta p_{zi} \right| < 0.00001,$$

it can be calculated by MATLAB that $r_A = 33$. Thus, the matrix A is column full rank, which means there are 33 independent variables. Therefore, it's not necessary to remove relevant variables.

To verify that considering joint stiffness can improve the accuracy of parameter identification, the compared experiment is taken which only considers 27 geometric parameters without

the joint stiffness. Using the proposed model to iteratively calculate, the results show that ΔP of both considering and non-considering joint stiffness verges to 0. The results of considering the stiffness and not considering the stiffness are shown in the Table IV.

To modify the data of last five groups in Table III, the results in Table IV are used. The comparison between theoretical data and modified data is shown in Figure 4. It is clear that the results calculated by the model considering the joint stiffness have smaller errors along all three directions than the non-considered one, which means the modified data are closer to the actual value where the error can be within 0.5 mm. Thus, with the loads, the model considering the joint stiffness can improve the absolute positioning accuracy remarkably. Moreover, from the figure, the results from the model not considering joint stiffness have larger differences, indicating the bad stability. On the contrary, the results from the model considering joint stiffness are more stable, having smaller differences in different positions. Also according to the calculation of the standard deviation, the model considering joint stiffness has better stability and smaller volatility.

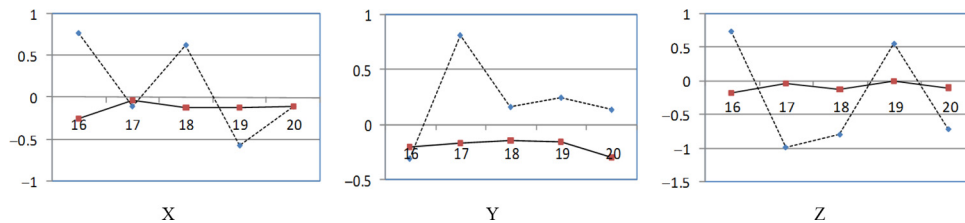
Table III The position of measured points

No.	$\theta_1(^{\circ})$	$\theta_2(^{\circ})$	$\theta_3(^{\circ})$	$\theta_4(^{\circ})$	$\theta_5(^{\circ})$	$\theta_6(^{\circ})$	$p_x(mm)$	$p_y(mm)$	$p_z(mm)$	$F_x(N)$	$F_y(N)$	$F_z(N)$
1	51.8876	-64.1974	31.2652	180.8670	-34.7215	-319.4809	501.2187	1,460.3168	2,650.7974	486.858	570.254	16.742
2	62.9244	-3.5251	55.0468	287.8476	-79.8006	-112.4795	-1,934.2742	-929.401	106.1919	-489.996	-472.616	314.703
3	47.7290	-4.8094	31.0728	314.3727	19.6290	-50.3342	747.1197	642.7241	-1,089.1321	-698.257	138.962	235.853
4	156.4787	-86.9572	72.1386	-204.8011	-54.2309	-152.7702	905.4033	-1,098.991	576.2688	65.627	745.481	49.516
5	-102.3094	-36.0818	26.1144	-240.1487	-103.8645	-201.4592	-686.2284	-319.5266	605.3495	355.361	-224.578	-621.115
6	73.5625	-40.5295	135.3407	130.5171	58.1248	213.9446	-52.3411	1,620.4519	58.9349	-721.377	-197.866	54.447
7	-92.7150	-46.4446	-44.3108	-270.1097	-58.6449	-46.6023	-229.7357	-684.7827	3,295.2156	650.937	-344.503	-141.769
8	-133.7822	0.4666	-70.4760	16.8939	-13.1323	257.8677	117.3119	-2,449.8263	-416.5125	198.759	494.390	-527.801
9	37.7173	-85.7690	-69.5721	20.1789	42.8175	-72.3633	-2,003.7123	-287.7133	441.2528	269.119	-694.934	-84.511
10	-17.5266	-78.1744	-80.2595	240.1580	-32.0960	178.9611	16.3885	992.646	984.5409	-253.999	701.855	-73.375
11	-14.5080	-106.5119	-1.2184	-10.0725	53.8855	-68.6336	-329.3199	-2,061.7682	382.5754	370.037	-6.172	2.114
12	56.9236	10.4257	8.9328	-70.8515	-24.0067	205.1619	-721.8295	-1,003.226	1,610.0954	6.102	-2.368	-3.662
13	95.0054	-31.5089	-10.2038	114.0017	41.8188	169.6263	1,200.1913	1,132.176	1,346.6274	-2.207	4.649	-5.456
14	-52.6484	-55.1765	81.9804	160.4365	46.5228	-81.5320	162.3543	375.1391	-829.4882	-5.592	-1.198	-4.853
15	56.9464	-32.3973	50.5464	13.3349	-13.1544	-188.8474	2,369.8822	559.102	1,691.4481	6.768	-1.144	-3.023
16	-16.2587	-120.6932	53.9811	23.6404	59.1152	18.2717	-101.2094	786.2615	3,343.3189	5.701	-2.228	-4.334
17	-147.3823	-85.2634	-78.0664	-273.5921	-117.5192	160.7966	298.3035	384.7125	120.5957	6.134	-3.939	1.761
18	183.2942	-123.0473	-80.2696	228.0662	-108.3726	145.0774	316.7298	-79.8154	293.6327	-6.935	-2.118	-1.916
19	-62.1257	-54.1858	89.6467	-113.3316	40.2999	196.9639	237.0330	-498.1911	548.5982	2.609	1.272	-6.915
20	-74.9817	-15.7861	120.8529	-144.2189	24.8323	-148.4161	914.4789	63.7062	725.0378	-6.257	-2.565	3.244

Table IV Calculated error parameters

i	$\Delta \theta_{i-1}/(^{\circ})$	$\Delta \theta_i(^{\circ})$	$\Delta \beta_{i-1}/(^{\circ})$	$\Delta d_i/(mm)$	$\Delta a_{i-1}/(mm)$	$k \theta_i(^{\circ})$	others
1	0.9151/0.9147	0.8166/0.8067	0.6793/0.6643	0.4163/1.3581	1.0858/1.0741	3.6122e9	Δty_0
2	-0.7911/-0.7953	0.9048/0.9282	/	/	0.9734/1.0467	2.6513e9	0.8775/0.8277
3	-0.9605/-0.9557	0.9412	0.9346/0.9285	0.4891/0.6767	-0.4349/-0.2737	3.5621e9	$\Delta t d_x$
4	0.6593/0.6565	0.9105/0.9554	/	-0.9680/-1.0116	0.8070/0.9041	2.6359e9	0.7310/0.5475
5	0.0364/0.0279	0.9709	/	0.9670/0.2143	0.1000/-0.2137	1.3969e9	
6	-0.8443/-0.8072	0.1014/0.0731	/	-0.1562/0.2093	0.3897/0.4632	1.3302e8	

Note: Considered stiffness/not considered

Figure 4 The comparison between actual data and rectified data (mm).—considering joint stiffness, ----not considering joint stiffness

6. Conclusion

The parameter identification is an important part of robot calibration, and an unneglectable positional error during calibration is the compliance error. To improve the positional accuracy, this study integrates the joint stiffness parameter into the geometric parameter identification model and proposes a more accurate model. To test the accuracy and performance of the proposed model, a calibration experiment on KUKA robot KR500-3 is performed, using mathematical model to process the data which are acquired via laser tracker. Comparing two kinds of results which one considers the joint stiffness and the other does not, the result indicates that the model considering joint stiffness can better reflect the actual condition of robot with better stability.

References

- Bo, Z., Xi, Z., Meng, Z. and Dai, X. (2014), "Off-line programming system of industrial robot for spraying manufacturing optimization", *The 33th Chinese Control Conference*, July 28.
- Chen, H.P., Fuhlbrigge, T., Choi, S., Wang, J.J. and Li, X.Z. (2008), "Practical industrial robot zero offset calibration", *IEEE International Conference on Robotics and Automation*, pp. 516-521.
- Chen, Y.S. (2011), *Joint Stiffness Identification of 6R Industrial Robot and Experimental Verification*, Huazhong University of Science and Technology.
- Chen, S.Y., Zhang, T. and Zou, Y.B. (2017), "Fuzzy-sliding mode force control research on robotic machining", *Journal of Robotics*, Vol. 2017 No. 1, pp. 1-8.
- Filion, A., Joubair, A., Tahan, A. and Bonev, I. (2018), "Robot calibration using a portable photogrammetry system", *Robotics and Computer-Integrated Manufacturing*, Vol. 49, pp. 77-87.
- He, X., Tian, W., Zeng, Y.F., Liao, W.H. and Xiang, Y. (2017), "Robot positioning error and residual error compensation for aircraft assembly", *Hangkong Xuebao/Acta Aeronautica et Astronautica Sinica*, Vol. 38 No. 4, pp. 292-302.
- Joubair, A., Tahan, A.S. and Bonev, I.A. (2016), "Performances of observability indices for industrial robot calibration", *IEEE/RSJ International Conference on Intelligent Robots and Systems*, pp. 23-26.
- Karan, B. and Vukobratovic, M. (2009), "A practical approach to enhance positioning accuracy for industrial robots", *ICROS-SICE International Joint Conference*, pp. 18-21.
- Liou, Y.H.A., Lin, P.P., Lindeke, R.R. and Chiang, H. (1993), "Tolerances specification of robot kinematic parameters using an experimental design technique—the taguchi method", *Robotics and Computer-Integrated Manufacturing*, Vol. 10 No. 3, pp. 199-207.
- Nubiola, A. and Bonev, I.A. (2013), "Absolute calibration of an ABB IRB 1600 robot using a laser tracker", *Robotics and Computer-Integrated Manufacturing*, Vol. 29 No. 1, pp. 236-245.
- Oh, Y.T. (2018), "Influence of geometric error on accuracy of industrial robot", *Journal of Engineering and Applied Sciences*, Vol. 13 No. 7, pp. 1877-1887.
- Ren, Y.J., Zheng, J.G., Yang, X.Y. and Ye, S.H. (2007), "Method of robot calibration based on laser tracker", *Chinese Journal of Mechanical Engineering*, Vol. 43 No. 9, pp. 195-199.
- Wang, J.J., Zhang, H. and Fuhlbrigge, T. (2009), "Improving machining accuracy with robot deformation compensation", *IEEE International Conference on Intelligent Robots and Systems*, pp. 11-15.
- Wang, Y., Liu, C.J., Ren, Y.J. and Ye, S.H. (2011), "Compensation for positioning error of industrial coordinate measurement robot", *Journal of Mechanical Engineering*, Vol. 15 No. 47, pp. 447-450.
- Wang, Z.X., Bai, J., Zhang, X.Y., Qin, X.S., Tan, X.Q. and Zhao, Y.L. (2018), "Base detection research of drilling robot system by using visual inspection", *Journal of Robotics*, Vol. 2018, pp. 1-9.
- Zhong, X.L. and Lewis, J.M. (1995), "A new method for autonomous robot calibration", *IEEE International Conference on Robotics and Automation*, Vol. 2, pp. 1790-1795.
- Ziegert, J. (1988), "Basic consideration for robot calibration", *IEEE International Conference on Robotics and Automation*, Vol. 2, pp. 932-938.

Corresponding author

Le Fan can be contacted at: fanle@mail.nwpu.edu.cn

For instructions on how to order reprints of this article, please visit our website:

www.emeraldgroupublishing.com/licensing/reprints.htm

Or contact us for further details: permissions@emeraldinsight.com